Hindawi
Advances in Civil Engineering
Volume 2021, Article ID 2275820, 12 pages
https://doi.org/10.1155/2021/2275820

Research Article

Mechanism and Control of Cable Breakage in a Roadway with Thick Top Coal in a Rockburst Mine

Ying Xu,[1] **Xiekang Zhou**,[1] **and Weimei Gong**[2]

[1]*School of Mines, China University of Mining and Technology, Xuzhou 221116, China*
[2]*Shandong Tian'an Mining Group CO., Ltd., Jining 273155, China*

Correspondence should be addressed to Ying Xu; kdxuying@163.com

Received 9 April 2021; Accepted 31 May 2021; Published 12 June 2021

Academic Editor: Zizheng Zhang

Because top coal is not stable, a roadway with thick top coal often appears to mine pressure problems, such as bolt failure, cable breakage, and roof caving. In particular, these problems are more serious in rockburst mines. Based on a cable breakage case of No. 3 roadway in Xingcun coal mine, the paper analyzed the stress and elastic energy evolution law of surrounding rock and stress state of cable in the 3# roadway by means of the numerical simulation method. Thus, the cable breakage mechanism of the roadway with thick top coal in rockburst mine was revealed. Then, because surrounding rock grouting can reduce the stress concentration of surrounding rock and cable, surrounding rock grouting technology was proposed as control technology of cable breakage. Finally, parameters of surrounding rock grouting were designed and applied in the No. 3 roadway. The field results showed that surrounding rock grouting technology can be one of the solutions for cable breakage of roadway with thick top coal in rockburst mine. The research results of this paper can provide certain theoretical and practical value for mine pressure control of roadway.

1. Introduction

In China, with the increase of coal seam mining depth and intensity, there are more and more rockburst mines. According to statistics of the China National Administration of Mine Safety, there are currently about 138 rockburst mines. In these rockburst mines, the problem of mine pressure is more serious. Through the research and implementation of occurrence mechanisms, hazard pre-evaluation, real-time monitoring, and early warning, comprehensive prevention, and control, most rockburst problems are gradually being resolved [1–6]. However, due to unclear mechanisms and inadequate control technology of rockburst under complex conditions, there are still some rockburst phenomena, events, and accidents.

According to the consequences of damage, rockburst can be divided into general rockburst (rockburst phenomenon), destructive rockburst (rockburst events), and accidental rockburst (rockburst accidents). Many engineers and scholars pay more attention to the last two rockburst types because of their more severe damage and more casualties. For instance, Zhu et al. [7] analyzed the rockburst accident in the first section of the working face of No. 3 and No. 4 mining area of layer 17, 3rd level north mining zone in Junde coalmine. Wu et al. [8] studied the occurrence of dynamic disasters during the horizontal sublevel mining of a steeply inclined and extremely thick coal seam in the Wudong coal mine. Yang [9] investigated rockburst accidents in some typical coal mines, and the behavior and predisposing factors of rockburst were analyzed. Li [10] analyzed several rockburst events and accidents of roadway floor in the Huating coalfield. Li et al. [11] studied the influence of geological and mining technology factors on the rockburst formation based on the analysis on the occurrence characteristics of rockburst in Qianqiu coal mine. Tian [12] researched the occurrence mechanism and prevention of rockburst of Xinzhouyao mine in Datong combining the mining condition and what type of rockburst happened. But the frequent occurrence of general rockburst (rockburst phenomenon) may be a precursor or gradually cause the occurrence of destructive rockburst (rockburst events) and accidental rockburst (rockburst accidents). Therefore, the

occurrence mechanism, characteristics, and prevention technology of general rockburst should also receive more attention, for example, high energy microseismic activity [13, 14], coal crack with firecrackers or thunder sound [15, 16], and breakage of bolt or cable [17, 18].

Cable breakage occurred frequently in the No. 3 roadway in Xingcun coal mine of Shandong Tian'an Mining Group CO., Ltd., during the roadway excavation. The paper aims at addressing the cause and solution of the case of general rockburst (rockburst phenomenon). Firstly, based on the analysis of stress and elastic energy evolution law of surrounding rock and stress state of cable, cable breakage mechanism was revealed. After that, grouting technology and parameters of cable breakage control were designed and applied in the No. 3 roadway. The research results can provide certain theoretical and practical value for mine pressure control of roadway, especially in rockburst mines.

2. A Case of Cable Breakage

2.1. Situation of Roadway. Xingcun coal mine, located in Jining city, is mining No. 3 coal seam with about 8.5 meters thick. Because of depth of more than 1100 m and many faults, initial ground stress is very high (Table 1). In addition, according to the appraisal report of rockburst tendency, the No. 3 coal seam and its roof have a weak rockburst tendency. So Xingcun coal mine is determined as a rockburst mine. The mine pressure on the working face and roadway appears to be severe. Particularly, there were several rockburst events in the past.

In the recent roadway excavation project, cable breakage occurred in the No. 3 exploration roadway in the seventh mining area of the Xingcun coal mine. The roadway adopted a straight wall circular arch section with 4300 mm width, 3000 mm straight wall height, and 700 mm circular arch height (Figure 1). Because it was driven along the floor of the coal seam, its roof was reserved with about 4.8 m top coal.

The support form of the No. 3 exploration roadway was bolt and cable support. The bolt was made of KMG500 heat-treated threaded steel with 22 mm diameter, 2400 mm length, and 180 kN anchoring force. The spacing and row spacing of bolts were 800 mm. In particular, 400 Nm pretightening torque was imposed on the bolts. The cable was a constant resistance cable of the H-MS-500-08 model with diameter of 22 mm, length of 8000 mm, constant resistance of 350 kN, and allowable deformation of 300 mm–500 mm [19, 20]. The spacing and row spacing of the cable was 800 mm. 250 kN pretightening force was imposed on the cable.

2.2. Situation of Cable Breakage. According to the field observations data that lasted for a month during the No. 3 roadway excavation, it was found that 34 cases of cable breakage (Figure 2) occurred in the range of 10 m~30 m from the heading of roadway and 9 cases of cable breakage occurred in the range of 30 m outside the heading. Among the 34 cases, all of them were roof cable, 15 cases on the arch of the roof, 12 cases on the right side of the roof, and 7 cases on the left side of the roof. Among the 9 cases, 6 cases, 2 cases, and 1 case of cable breakage occurred on the arch of roof, the left side of the roof, and the right side of the roof, respectively.

In addition, the cable breakage had the following characteristics:

(1) When a fully mechanized excavating machine was driving or coal cracked with firecrackers or thunder sound, which were two sources of dynamic load, the cable breakage occurred.

(2) From the analysis of the shape and characteristics of the cable breakage, it can be judged as a "tension-shear" breakage.

(3) The cable breakage was mainly concentrated between 1.5 m and 3.5 m away from the anchorage of the cable.

(4) The constant resistors of cable were deformed and the constant resistance displacement was 0~200 mm which was less than the allowable deformation of cable.

2.3. Deformation of Top Coal. During the No. 3 roadway excavation, the top coal and rock of the roof were drilled and peeped at 15 m behind the heading of the roadway. From the peeping images of the boreholes (Figure 3), it can be seen that the top coal between 1.6 m and 4.0 m had poor integrity, severe separation, loose and broken parts, and well-developed fissures; vertical fissures between 4.0 m and 4.8 m were developed in the top coal. But the rock of the roof in 4.8 m~6.2 m had better integrity. In general, the thick top coal of the No. 3 roadway was damaged and loose, but the rock above top coal was more stable. In other words, the thick top coal of roadway was mainly deformed and difficult to control surrounding rock, which was like other thick top coal roadways in other coal mines [21, 22].

3. Cable Breakage Mechanism

3.1. Stress Evolution Law of Roof. The cable stress was the foundation of cable breakage. Therefore, the mechanism of cable breakage can be revealed by clarifying the causes and changes of cable stress. According to the interaction between anchor cable and surrounding rock [23], the reason for cable stress was the deformation of surrounding rock. Therefore, this paper firstly analyzed the stress evolution law of surrounding rock by numerical simulation method.

A three-dimensional numerical simulation model of the No. 3 roadway was established using FLAC3D software (Figure 4). The horizontal width, strike length, and vertical height of the model were $X \times Y \times Z = 50\,\text{m} \times 30\,\text{m} \times 47.5\,\text{m}$. For the accuracy of calculation, the grids of adjacent roadways were densely divided, and other grids were relatively sparse. The total number of nodes was 226,414 and the total number of units was 214,800. The front, rear, left, right, and top surfaces of the model used a stress boundary, and initial ground stresses (Table 1) were applied on the surfaces. The bottom surface used displacement boundaries. The

Table 1: Initial ground stress of Xingcun coal mine.

		σ Maximum principal stress			σ Intermediate principal stress			σ Minimum principal stress		
Measuring point	Depth (m)	Value (MPa)	Direction (°)	Inclination (°)	Value (MPa)	Direction (°)	Inclination (°)	Value (MPa)	Direction (°)	Inclination (°)
No. 1	−1186	68.46	152.86	8.35	49.63	−115.07	13.86	35.23	−147.35	−73.73
No. 2	−1156	68.65	153.87	10.26	54.69	65.57	7.16	34.92	121.25	−77.44

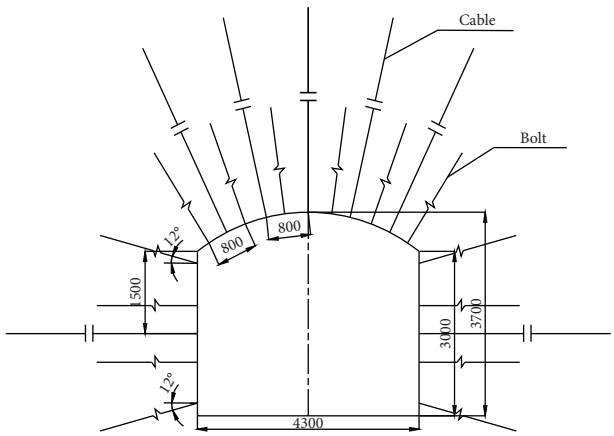

Figure 1: Section size and support parameters of No. 3 exploration roadway (unit: mm).

Mohr-Coulomb constitutive model was used for the constitutive relationship of coal and rock, and Table 2 showed their mechanical parameters.

The excavation of the roadway made the surrounding rock lose the original equilibrium state and caused the stress redistribution within a limited range; that is, the stress in the surrounding rock had a continuous change process in time and space [24]. For the stress evolution in space, the surrounding rock within 10 meters above the roadway arch was selected for stress monitoring. For the stress evolution in time, the roadway advancing was simulated by the step-by-step excavation method, and the step advancing distance was 3 m.

According to the numerical simulation results (Figure 5), horizontal stress evolution law was as follows:

(1) When the roadway was excavated forward 3 m, the horizontal stress peak in the same cross-section of the roof was 35.45 MPa. When the roadway was excavated forward 9 m, the peak stress was 38.54 MPa. When the roadway was excavated forward 18 m, the peak stress was 39.42 MPa. In a word, horizontal stress peak in the same cross-section of the roof had a tendency to increase with the roadway excavation.

(2) When the roadway was excavated forward 6 m, horizontal stress peak was located at 2.5 m in the top coal. When the roadway was excavated forward 15 m, horizontal stress peak was located at 3.0 m in the top coal. In a word, horizontal stress peak shifts to deep with the roadway excavation.

In addition, according to the numerical simulation results (Figure 6), vertical stress evolution laws were as follows: when the roadway was advanced for 3 m, the vertical stress peak was 64.69 MPa. When the roadway was advanced for 9 m, the vertical stress peak was 57.35 MPa. When the roadway was advanced for 18 m, the vertical stress peak was 55.43 MPa. In a word, with the roadway advancing, the vertical stress peak at the same position of the roadway roof gradually decreases.

From the perspective of the evolution law of horizontal and vertical stress on the roof of the roadway, as the roadway excavation, the horizontal stress peak increased and finally tended to balance and shifted to the deep. Particularly the horizontal stress peak no longer spread to the deep when it was transferred to a depth of about 3 m in top coal. But the vertical stress peak gradually decreases as the roadway advances and eventually tends to balance. This causes the stress difference between the horizontal and vertical stress to gradually increase as the roadway excavation continues. The maximum stress difference occurred at about 3.5 m in depth in top coal, which was about the place of cable breakage.

3.2. Elastic Energy Evolution Law of Roof. The change of elastic energy in the surrounding rock of roadway was the main cause of rockburst phenomenon, incident, or accident in a roadway [25–28]. The elastic energy of surrounding rock of roadway is

$$E_0 = \frac{\left[\sigma_1^2 + \sigma_2^2 + \sigma_3^2 - 2\mu\left(\sigma_1\sigma_2 + \sigma_1\sigma_3 + \sigma_3\sigma_2\right)\right]}{2E}, \quad (1)$$

where E is the modulus of elasticity, M is Poisson's ratio, σ_1 is the maximum principal stress, σ_2 is the intermediate principal stress, and σ_3 is the minimum principal stress.

Based on the numerical simulation model shown in Figure 4, the elastic energy evolution law of the roof was obtained (Figure 7). The following can be seen:

(1) The elastic energy of the shallow surrounding rock was released instantly after the roadway was excavated, and the elastic energy accumulated in the deep coal and rock. In particular, the elastic energy accumulation range was between 3 m and 4 m in depth in the top coal.

(2) As the roadway excavation, the elastic energy in the range of 10 m in depth of roof was released, and when the roadway advanced distance changed from 3 m to 6 m, the elastic energy released at the area around 3.5 m in depth in the top coal was the largest. The position was exactly the place of cable breakage.

3.3. Cable Stress Distribution. The force of the cable that exceeded the ultimate strength of the anchor cable was the most direct cause of cable breakage. Based on the numerical

Figure 2: Cable breakage of No. 3 exploration roadway.

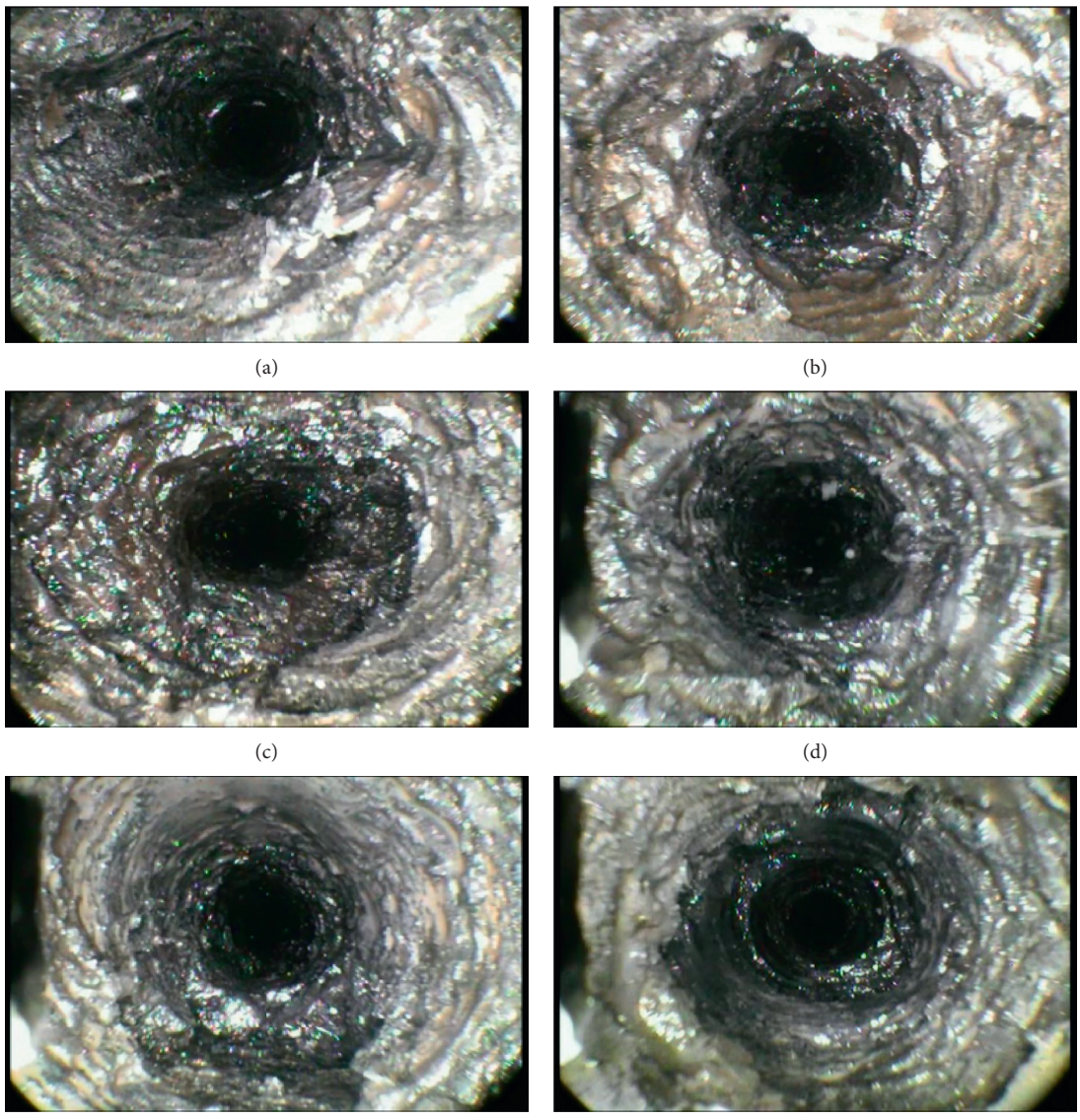

(a) (b) (c) (d) (e) (f)

Figure 3: Continued.

(g)

Figure 3: Borehole peep image under different borehole depths. (a) 1.6 m. (b) 2.5 m. (c) 3.1 m. (d) 4.0 m. (e) 4.3 m in depth. (f) 4.8 m in depth. (g) 6.2 m in depth.

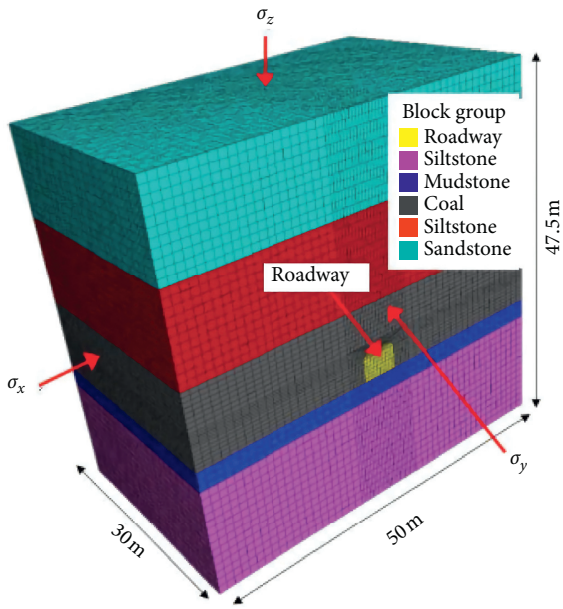

Figure 4: Three-dimensional numerical simulation model of the No. 3 roadway.

simulation model shown in Figure 4, cable stress distribution under different excavation distances of roadway was obtained (Figure 8). The following can be seen:

(1) Whether the roadway excavation distance was 3 m, 6 m, 9 m, and 12 m, the cable stress increased first and then decreased from the surface to the deep part of the top coal and the rock, and the concentrated part of the larger axial force of the cable was within the range of 2 m~4 m.

(2) When the roadway was advanced for 3 m, 6 cables with an axial force greater than 1.4×10^6 MPa appeared. When the roadway advanced for 9 m, 12 cables with an axial force greater than 1.4×10^6 MPa appeared. When the roadway advanced for 12 m, there were 14 cables with an axial force greater than 1.4×10^6 MPa, which was 2 times more than that which appeared when the roadway advanced for 9 m. In a word, as the roadway advanced, more and more cables with an axial force greater than 1.4×10^6 MPa appeared.

(3) Because the length of the bolt was 2.4 m which was in the top coal range, blot stress was uniform and little change as the roadway excavation. In other words, the bolts of the roof were not broken, but the cable was broken. The roadway scene also proved the phenomenon.

Through the above analysis of stress distribution, elastic energy distribution, and cable stress, cable breakage mechanism was revealed: in the process of roadway excavation, the stress was constantly redistributed and the stress was constantly shifting to the deep part of the roof. The vertical stress dropped at about 3.5 m in depth in top coal of the roadway with a large descending gradient, and the horizontal stress reached its peak. Especially when the surrounding rock in the load-bearing area suddenly broke, due to the large amount of elastic energy that accumulated here, the surrounding rock in this area would be dislocated instantly, and the cable would be broken in the area where the axial force was concentrated.

4. Control of Cable Breakage

4.1. Control Mechanism of Surrounding Rock Grouting. Surrounding rock grouting technology can allow the grout to penetrate the fissures in the surrounding rock, thereby improving the integrity, elastic modulus, and strength of the surrounding rock. In addition, it can transform the two-dimension force-bearing fractured structural surface due to the influence of excavation or mining into three-dimension force-bearing [29–31]. The following was a comparative analysis on the stress distribution of surrounding rock, the elastic energy of surrounding rock, and stress distribution of cable before and after surrounding rock grouting.

4.1.1. Comparison of Horizontal Stress Evolution. The mechanical parameters of the top coal and the rock with grouting were set larger than that without grouting in the numerical simulation model shown in Figure 4. Figure 9 was a comparison of the calculation results of horizontal stress

Table 2: Mechanical parameters of coal and rock.

Lithology	Density/kg·m^{-3}	Bulk modulus/GPa	Shear modulus/GPa	Friction/°	Cohesion/MPa	Tensile strength/MPa
Sandstone	2620	20.5	12.5	39	13	2.5
Siltstone	2640	16.1	10.2	35	12	1.9
Coal	1800	14.3	8.2	38	8	1.2
Mudstone	2490	15.6	8.8	36	11	2.2
Siltstone	2660	18.2	11.2	35	12	1.9

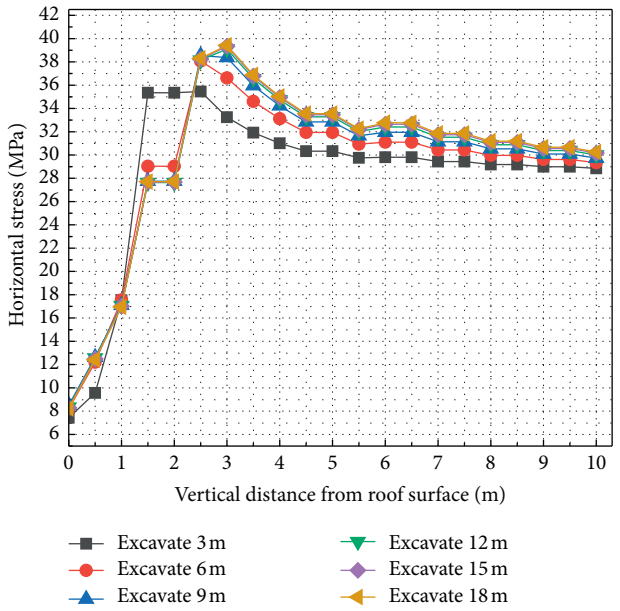

Figure 5: Horizontal stress distribution under different excavation distance.

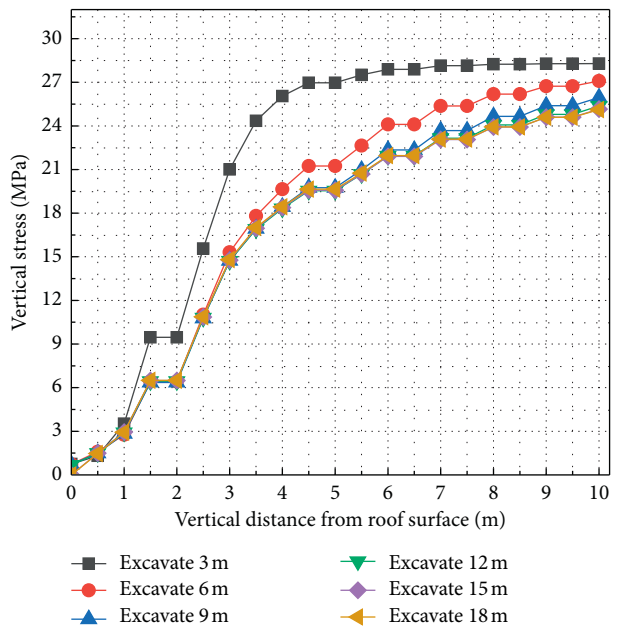

Figure 6: Vertical stress distribution under different excavation distance.

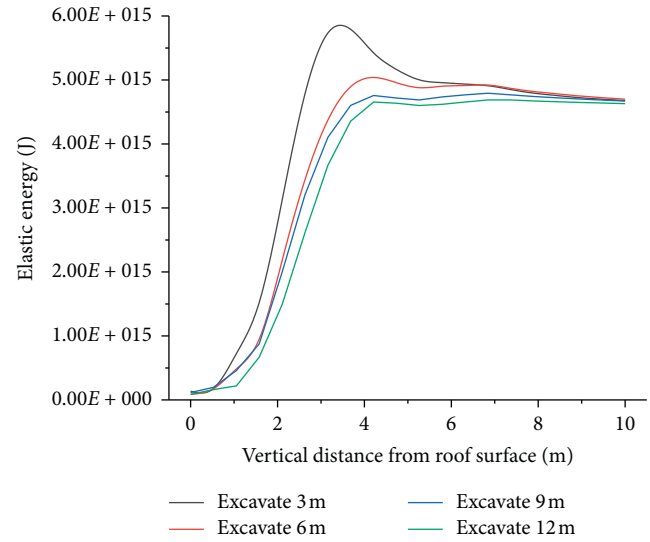

Figure 7: Elastic energy distribution under different excavation distance.

evolution. After surrounding rock grouting, the horizontal stress in the range of 0.5 m~3.5 m of the roof was relatively uniform. In addition, as the roadway excavation continues, the horizontal stress of the roof surface was continuously decreasing, which was consistent with the evolution law before surrounding rock grouting, but the difference was that the stress value of the roof surface did not appear to be greatly reduced and approached lower value but gradually approached the higher stress value after surrounding rock grouting.

4.1.2. Comparison of Vertical Stress Evolution. Figure 10 shows a comparison of the calculation results of vertical stress evolution. Whether it was grouted or not, as the roadway excavation continues, the vertical stress within 10 m above the roof surface gradually decreased as a whole. But compared to that without surrounding rock grouting, the vertical stress drops evenly within the range of 3 m~4 m of roof after surrounding rock grouting, and there was no instantaneous sharp drop in the vertical stress. Another aspect, regardless of whether there is surrounding rock grouting or not, as the roadway excavation continues, the vertical stress of the surrounding rock within 1 m above the roof surface was gradually decreasing, but there was no situation that the vertical stress tended to be of very low value without surrounding rock grouting. For example, at the part 1 m deep of the top coal, the vertical stress without

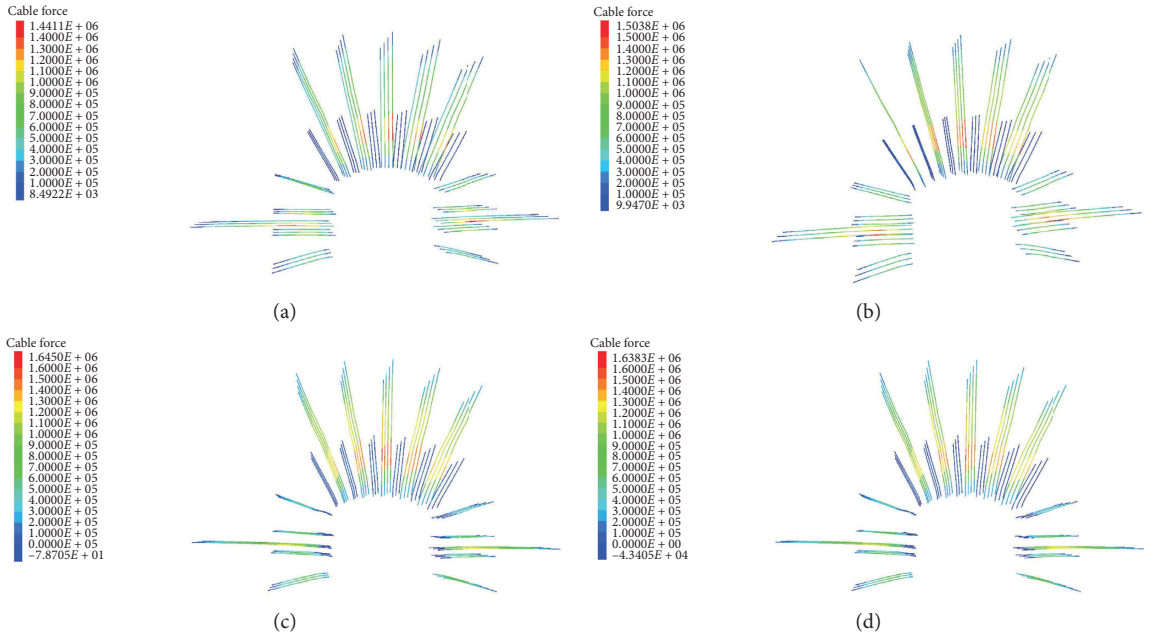

Figure 8: Stress condition of cable under different excavation distance. (a) Excavate 3 m. (b) Excavate 6 m. (c) Excavate 9 m. (d) Excavate 12 m.

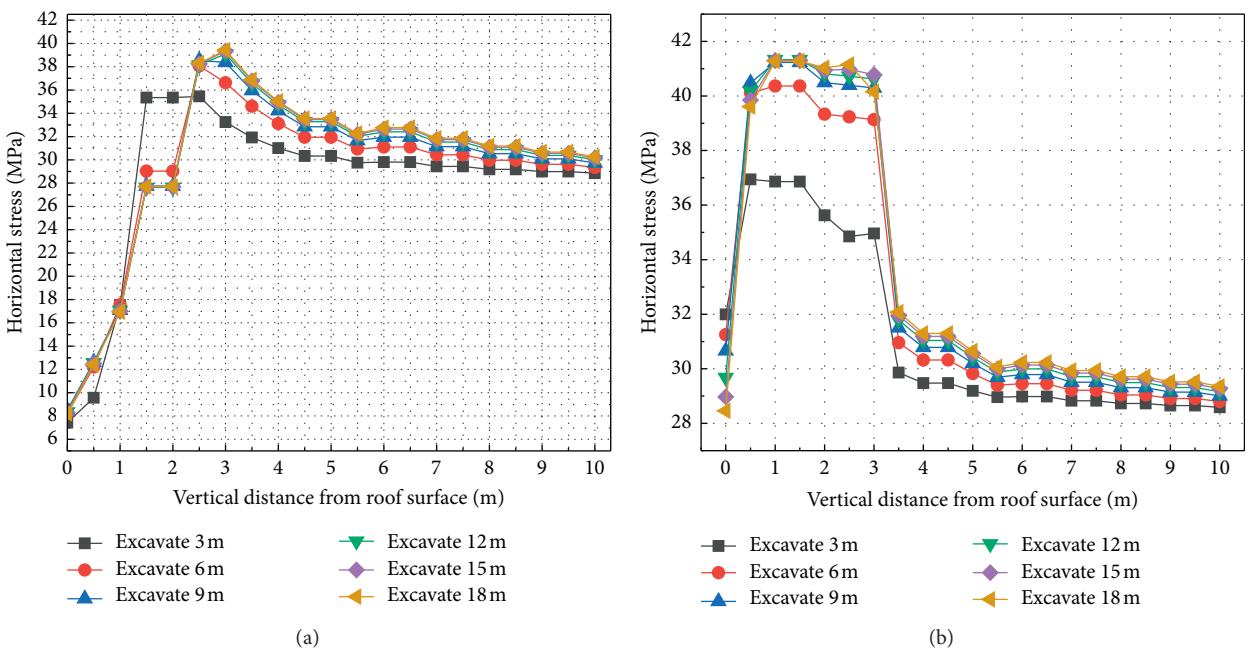

Figure 9: Horizontal stress evolution under different excavation distance without and with surrounding rock grouting. (a) Without surrounding rock grouting. (b) With surrounding rock grouting.

surrounding rock grouting was about 3 MPa, and the vertical stress was at 9 MPa after surrounding rock grouting.

4.1.3. Comparison of Elastic Energy Evolution. Figure 11 was a comparison of the calculation results of the elastic energy. When the roadway surrounding rock was not grouted, as the roadway excavation, the elastic energy of the surrounding rock within 1 m of the shallow part of the roof tended to zero, and a large amount of elastic energy accumulated within 3 m~4 m of the roof. After the surrounding rock was reinforced by grouting, although the surrounding rock energy was dissipated within 1 m of the shallow part of the roof, the elastic energy dissipation in this range was less compared to that without surrounding rock grouting. In addition, the elastic energy distribution of the surrounding rock was even within the range of 1.8 m~3 m of the roof, and the peak value was reduced compared to that without

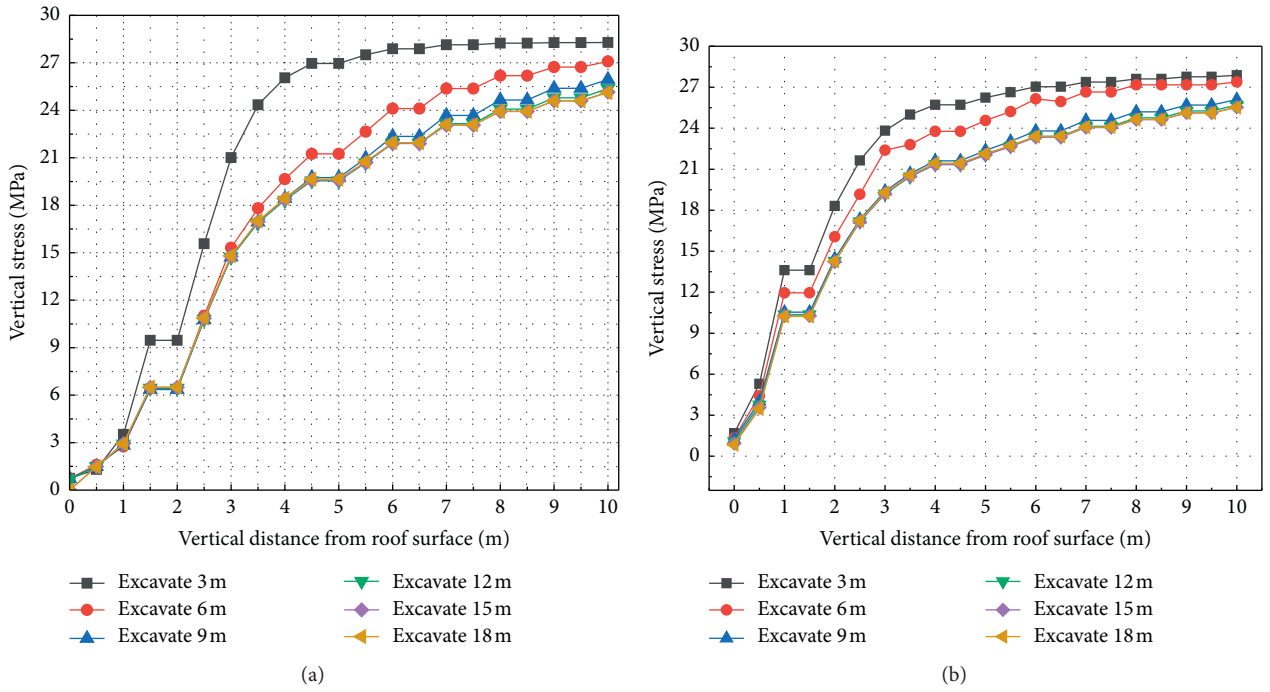

Figure 10: Vertical stress evolution under different excavation distance without and with surrounding rock grouting. (a) Without surrounding rock grouting. (b) With surrounding rock grouting.

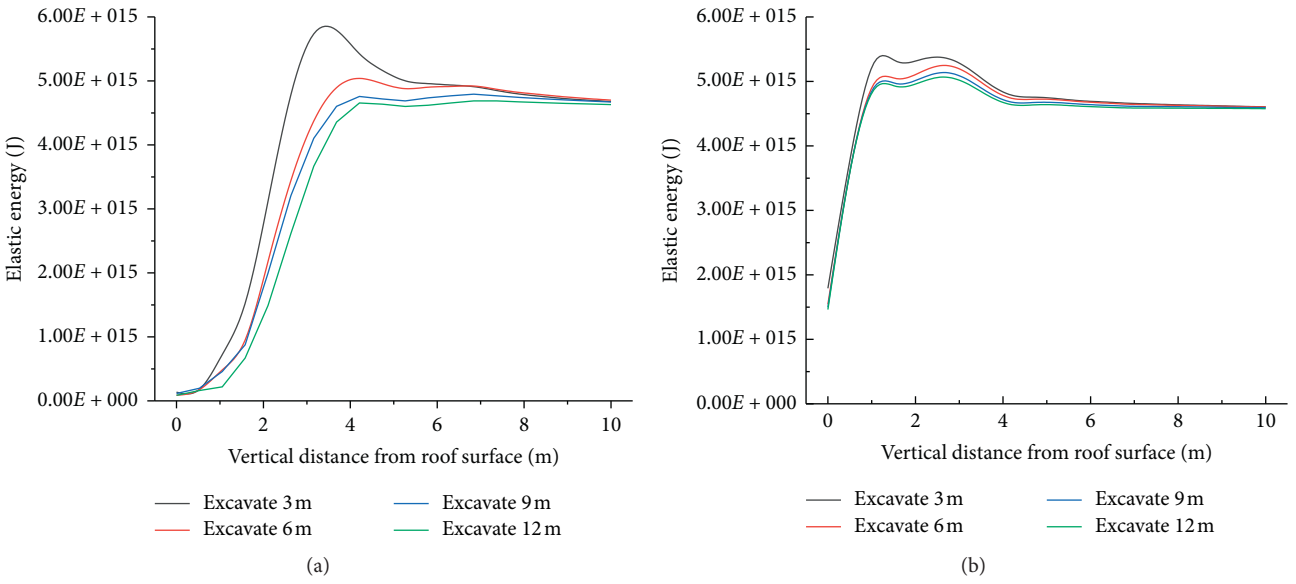

Figure 11: Elastic energy evolution under different excavation distance without and with surrounding rock grouting. (a) Without surrounding rock grouting. (b) With surrounding rock grouting.

surrounding rock. As the roadway excavation, the degree of the elastic energy dissipation in this range was smaller and even than that without surrounding rock grouting.

4.1.4. Cable Stress Distribution after Surrounding Rock Grouting. Cable stress distribution after surrounding rock grouting under different roadway excavation distance was obtained (Figure 12). Compared with that without surrounding rock grouting (Figure 8), the following can be seen:

(1) After the surrounding rock was grouted, the cable was uniformly stressed in the middle, and there was no axial force concentration, and the value was smaller than that without surrounding rock grouting.

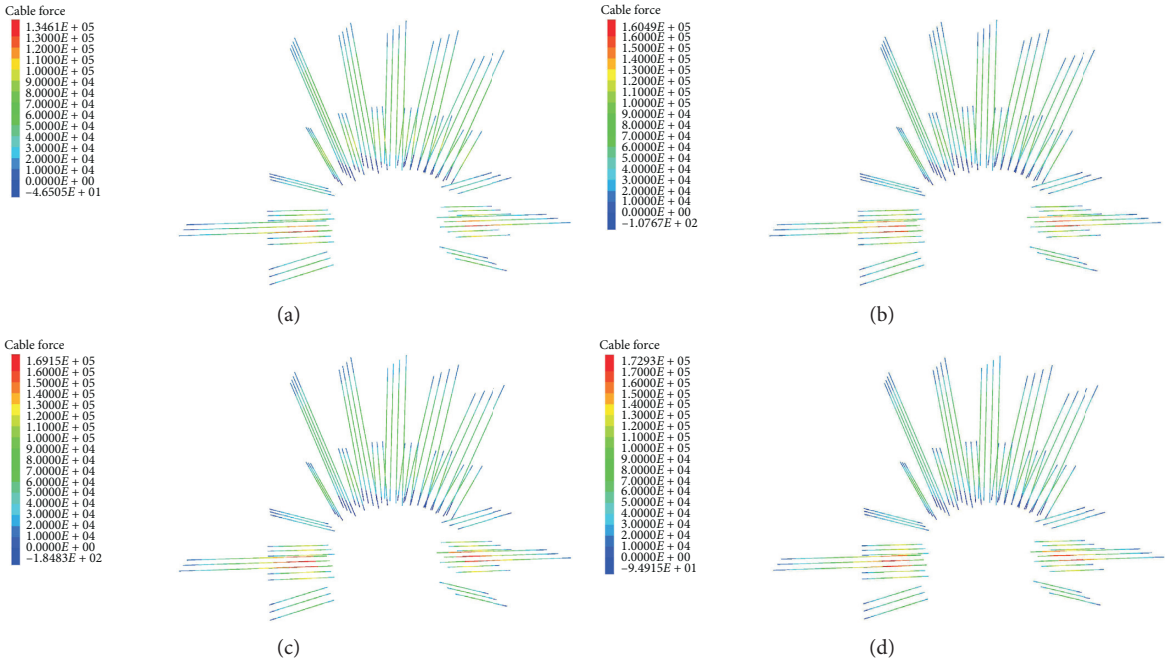

Figure 12: Cable stress distribution under different excavation distance with surrounding rock grouting. (a) Excavate 3 m. (b) Excavate 6 m. (c) Excavate 9 m. (d) Excavate12 m.

(2) After the surrounding rock was grouted, the cables with larger axial force were rib cables, but the maximal axial stress value of the rib cables was still smaller than that without surrounding rock grouting.

Through the above analysis, surrounding rock grouting can reduce the stress concentration of surrounding rock and cable. So surrounding rock grouting technology was proposed as control technology of cable breakage.

4.2. Parameters of Surrounding Rock Grouting

4.2.1. Grouting Material. According to the above borehole peeking results of the No. 3 roadway, it can be seen that the top coal of the roadway was loose and broken, and cracks were developed. So cement-based grouting material can be selected for surrounding rock grouting of the roadway [32]. Particularly, the grouting material had a wide source and low price. The water-cement ratio was 0.8 : 1.

4.2.2. Grouting Hole Design. The reasonable design of surrounding rock grouting holes can effectively shorten the work, reduce the number of grouting materials, and increase the utilization rate of the grout. The grouting method of the No. 3 roadway used a combination of shallow hole grouting and deep hole grouting (Figure 13). The length of the shallow hole grouting pipe was 2600 mm (in the range of the fissure development zone), the radius was 15 mm, and the spacing and row spacing were 1300 mm. The length of the deep hole grouting pipe was 4800 mm (in the range of the small fissure zone), the radius was 10 mm, and the spacing and row spacing were 1300 mm.

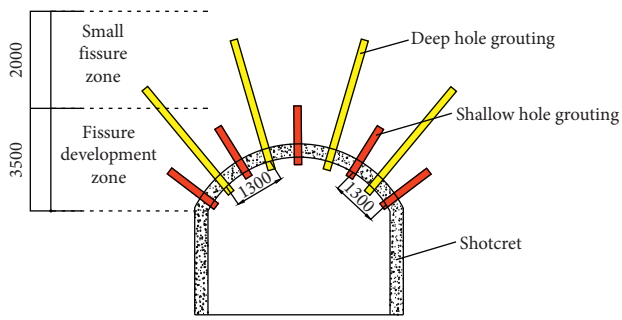

Figure 13: Schematic diagram of grouting hole design (unit: mm).

4.2.3. Grouting Pressure. The pressure selected for surrounding rock grouting was to ensure that the grout can penetrate the fissures of the surrounding rock, but the grouting pressure should not be too high or too small [33]. If the grouting pressure was too high, problems such as roof falling will easily occur. If the grouting pressure was too small, the grout cannot be diffused in the surrounding rock due to insufficient power, and the grouting cannot achieve the expected effect of reinforcement. So the shallow hole grouting of the surrounding rock of the No. 3 roadway used 1 MPa grouting pressure, and the deep hole grouting used 1.5 MPa grouting pressure.

4.2.4. Shotcrete. The cement of concrete strength grade C20 was used to shoot out the surface of the No. 3 roadway to close the fissure on the surface of the surrounding rock of the roadway to ensure that the injected grout will not flow out and to improve the grouting efficiency and effect. The water-cement ratio was 0.5, and the thickness of the shotcrete was 60 mm.

5. Application

In order to verify the control effect of surrounding rock grouting technology on cable breakage, the design parameters were applied to the new excavation section of No. 3 roadway in Xingcun coal mine and the displacement of the surrounding rock and the cable force were monitored.

In the early stage of roadway excavation, the surface displacement of the surrounding rock near the heading of the roadway changes quickly. When the excavation distance was about 20 m from the heading, the surface displacement of the roadway started to converge stably. The convergence displacement of the two ribs was stabilized at about 53 mm, and the convergence displacement of the roof and floor was stabilized at about 97 mm (Figure 14). The deformation of the roadway was small.

In order to check the integrity of the surrounding rock of the roadway after grouting, deep base point displacement meters were used to monitor the displacement of the surrounding rock of the roadway at different depths. The first measuring point was arranged at a distance of 5 m from the heading of the roadway, and the next measuring point was arranged every 20 m of the roadway. There were 3 measuring points in total, and the average value of the displacement value of the same depth measured by each measuring point was regarded as the final result. Figure 15 showed that when the measuring point was close to the heading, the displacement of each depth of the roof of the roadway increased faster and finally stabilized gradually. According to the data, the amount of separation in the deep part of the surrounding rock of the roadway was smaller, and the shallow part was slightly larger. But after a certain period of time, they all tend to be stable, and the maximum displacement was on the surface of the roadway. The maximum displacement of the roof was 38 mm.

For the monitoring of the force of cable, the force of each part of the cable decreased first, then increased, and then stabilized (Figure 16). The axial force of the cable on the roof arch was the largest, and the maximum was 190.6 kN. The axial force of cable at the corner of the roadway was the next, and the maximum was 171.5 kN, and the anchoring force of the cable at the rib was the smallest, and the maximum was 151 kN. The axial force value of all the cable did not exceed the ultimate strength of the cable. More importantly, there was no cable breakage.

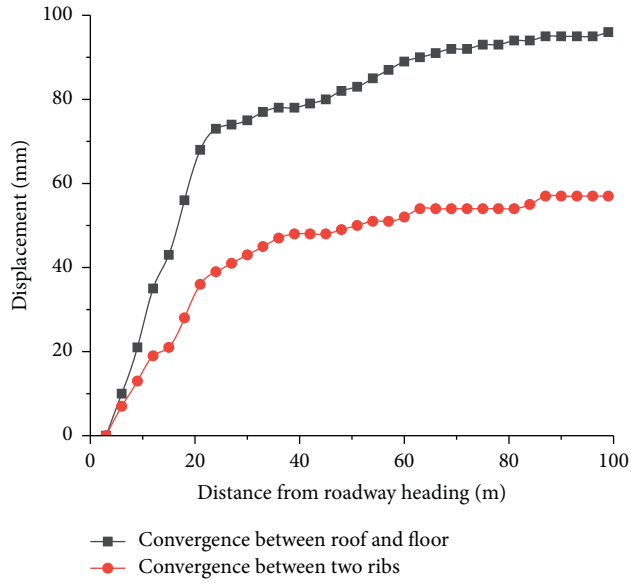

Figure 14: Convergence displacement of roadway surrounding rock surface in the No. 3 roadway.

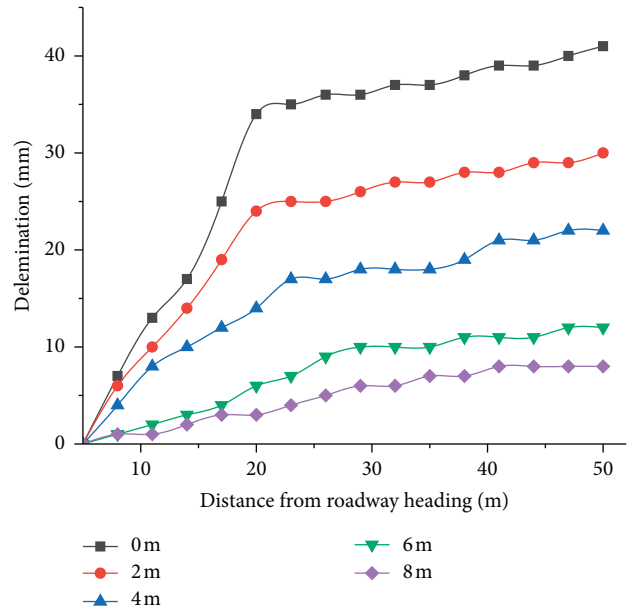

Figure 15: Displacement of surrounding rock at different depth in the No. 3 roadway.

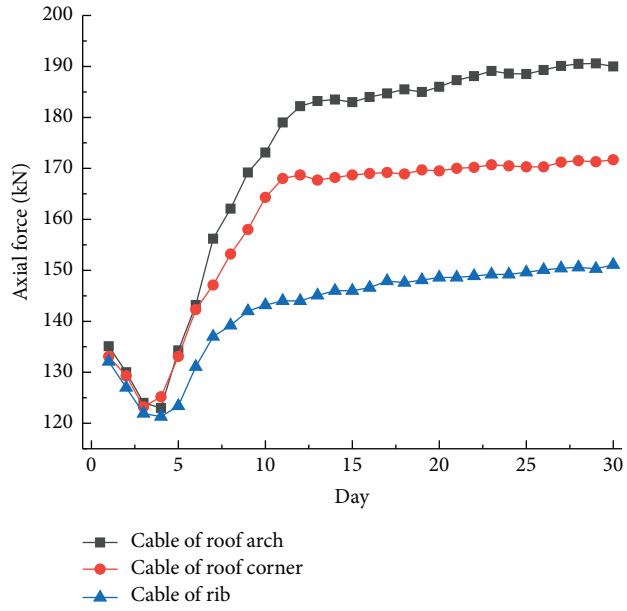

Figure 16: Axial force of the cable in the No. 3 roadway.

6. Conclusion

The study was mainly focused on the mechanism and control of the case of cable breakage in the No. 3 exploration roadway in Xingcun coal mine. The main conclusions in this paper are summarized as follows:

(1) When the roadway was excavated forward, there was a stress adjustment process in which the horizontal stress continuously increases and the vertical stress continuously decreases in the surrounding rock. The location of the largest difference between the horizontal stress and the vertical stress was about the position where the maximum axial force and breakage of cable occurred.

(2) When the roadway was excavated forward, the elastic energy of the surrounding rock was released from shallow part to deep part of roof and accumulated in the top coal at a depth of 3 m-4 m. The top coal and its accumulated elastic energy were the main factors of cable breakage.

(3) When the roadway was affected by dynamic load, a large amount of accumulated elastic energy in the top coal was released, and then the cable was broken at the position of maximum axial force.

(4) The surrounding rock grouting technology can make top coal improve the stress and elastic energy distribution, which was conducive to the uniform force of the cable and the prevention of cable breakage. The results of the field measurements of the No. 3 roadway showed there was no cable breakage phenomenon and guaranteed the normal use of the No. 3 roadway.

Data Availability

The data used to support the findings of this study are included within the article.

Conflicts of Interest

The authors declare that they have no conflicts of interest.

Acknowledgments

The financial support by the Fundamental Research Funds for the Central Universities (2020ZDPYMS16) and A Project Funded by the Priority Academic Program Development of Jiangsu Higher Education Institutions for this work are gratefully acknowledged.

References

[1] Q. Qi and L. Dou, *Theory and Technology of Rockburst*, China University of Mining and Technology Press, Xuzhou, China, 2008.

[2] L. Dou, S. Wang, S. Gong et al., "Cloud platform of rock-burst intelligent risk assessment and multi-parameter monitoring and early warning," *Journal of China Coal Society*, vol. 45, no. 6, pp. 2248–2255, 2020.

[3] Q. Qi, S. Zhao, H. Li et al., "Several key problems of coal bump prevention and control in china's coal mines," *Safety in Coal Mines*, vol. 51, no. 10, pp. 135–143, 2020.

[4] F. Jiang, Y. Liu, Y. Zhang, J. Wen, W. Yang, and J. An, "A three-zone structure loading model of overlying strata and its application on rockburst prevention," *Chinese Journal of Rock Mechanics and Engineering*, vol. 35, no. 12, pp. 2398–2408, 2016.

[5] S. Wang, W. Ju, J. Pan, and C. Lu, "Mechanism of energy partition evolution of excavation roadway rockburst in coal seam under tectonic stress field," *Journal of China Coal Society*, vol. 44, no. 7, pp. 2000–2010, 2019.

[6] Y. Pan, L. Dai, G. Li et al., "Study on compound disaster of rockburst and roof falling in coal mines," *Journal of China Coal Society*, vol. 46, no. 1, pp. 112–122, 2021.

[7] S. Zhu, Y. Ma, F. Jiang et al., "Mechanism of rockburst in the bottom coal seam of super high seam with overall slippage and instability," *Journal of Mining & Safety Engineering*, vol. 38, no. 1, pp. 31–40, 2021.

[8] Z. Wu, P. Pan, S. Zhao et al., "Study on the mechanism of rockbursts caused by "roof-rock pillar" in mining steeply-inclined and its prevention and treatment," *Journal of China Coal Society*.

[9] Y. Yang, *Mechanism and Prevention Technology of Coal Bumps for Highly-Stressed Coal in Deep Mining Under Dynamic Disturbance*, China University of Mining & Technology, Beijing, China, 2016.

[10] P. Li, *Study on Bursting Mechanism of Gateways Floor and Protection Methods in Huating Coal Field*, University of Science and Technology Beijing, Beijing, China, 2015.

[11] B. Li, W. Xiangzhi, and Y. Ren, "Analysis on occurrence characteristics and causes of rockburst in qianqiu coal mine," *Coal Engineering*, vol. 46, no. 1, pp. 83–86, 2014.

[12] L. Tian, *Research on the Occurrence Mechanism and Prevention of Compression Type Rockburst in Xinzhouyao Mine*, Liaoning Technical University, Fuxin, China, 2013.

[13] C. Dong, E. Wang, and L. Nan, "Analysis of microseismic source parameters and focal mechanism in qianqiu coal mine," *Journal of China Coal Society*, vol. 44, no. 7, pp. 2011–2019, 2019.

[14] X. Tian, Z. Li, and D. Song, "Study on microseismic precursors and early warning methods of rockbursts in a working face,"

Chinese Journal of Rock Mechanics and Engineering, vol. 39, no. 12, pp. 2471–2482, 2020.

[15] X. Du, Y. Jiang, and T. Wang, "Temporal and spatial distribution of rockburst in China," *Safety in Coal Mines*, vol. 48, no. 8, pp. 186–189, 2017.

[16] J. Wang, B. Li, and T. Zhang, "Research of action range and mechanism of coal-gun phenomenon in drifting process," *Industry and Mine Automation*, vol. 33, no. 7, pp. 39–41, 2010.

[17] H. Jing, J. Wu, Q. Yin et al., "Particle flow simulation of rockburst and roof fall of deep coal roadway under dynamic disturbance," *Chinese Journal of Rock Mechanics and Engineering*, vol. 39, pp. 3475–3487, 2020.

[18] A. Wang, Y. Pan, and B. Zhao, "Numerical analysis on the failure mechanism of bolted rock structure under impact load," *China Earthquake Engineering Journal*, vol. 39, no. 3, pp. 417–424, 2017.

[19] M.-C. He, J. Wang, X.-M. Sun, and X.-J. Yang, "Mechanics characteristics and applications of prevention and control rockbursts of the negative poisson's ratio effect anchor," *Journal of China Coal Society*, vol. 39, no. 2, pp. 214–221, 2014.

[20] G. Zhang, E. Wang, and L. Xu, "Mechanical characteristics of high constant resistance and large deformation anchor rope in coal mines," *Chinese Journal of Rock Mechanics and Engineering*, vol. 35, no. 10, pp. 2033–2043, 2016.

[21] L. Lei, *Research on the Catastrophe Mechanism and Control Technology of Roadway with Large Cross Section and Top Coal*, China University of Mining and Technology, Xuzhou, China, 2013.

[22] Y. Peng, J. Yang, J. Cheng et al., "Deformation mechanism and control technology of large section gateway with top coal in coal mine," *Journal of Mining Science and Technology*, vol. 2, no. 5, pp. 439–448, 2017.

[23] J. Hu, M. He, Z. Li et al., "Numerical study on NPR cable-rock interaction using 3D discrete-continuous coupling method," *Engineering Mechanics*, vol. 37, no. 7, pp. 27–34, 2020.

[24] Z. Zhang, *The Study on Temporal and Spatial Evolution Characteristics of Surrounding Rock Stress Shell of Deep Roadway and Supporting Mechanism*, China University of Mining & Technology, Beijing, China, 2018.

[25] S.-T. Zhu, F.-X. Jiang, X.-Y. Wang et al., "Energy accumulation characteristics and rockburst mechanism of surrounding rock at heading face of extra-thick coal seam," *Chinese Journal of Geotechnical Engineering*, vol. 41, no. 11, pp. 2071–2078, 2019.

[26] J. Yang, *Study on Evolutionary Mechanism of Energy Field and Support Mechanism of Energy-Absorbing Bolt in Deep Roadway*, University of Science and Technology Beijing, beijing, China, 2020.

[27] Y. Hui, X. Zhang, B. Li et al., "Macro-micro mechanical response and energy mechanism of surrounding rock under excavation disturbance," *Journal of China Coal Society*, vol. 45, no. S1, pp. 60–69, 2020.

[28] Y. Zhao, Y. Jiang, and S. Tian, "Investigation on the characteristics of energy dissipation in the preparation on the characteristics of energy dissipation in the preparation process of coal pumps," *Journal of China Coal Society*, vol. 35, no. 12, pp. 1979–1983, 2010.

[29] C. Hou, X. Wang, J. Bai et al., "Basic theory and technology study of stability control for surrounding rock in deep roadway," *Journal of China University of Mining & Technology*, vol. 50, no. 1, pp. 1–12, 2021.

[30] H. Kang, P. Jiang, B. Huang et al., "Roadway strata control technology by means of bolting-modification-destressing in synergy in 1000 m deep coal mines," *Journal of China Coal Society*, vol. 45, no. 3, pp. 845–864, 2020.

[31] A. Fahimifar and M. Ranjbarnia, "Analytical approach for the design of active grouted rockbolts in tunnel stability based on convergence-confinement method," *Tunnelling and Underground Space Technology*, vol. 24, no. 4, pp. 363–375, 2009.

[32] D. Ma, "Experimental research on optimum proportioning of coal cement grouting materials," *Coal*, vol. 25, no. 8, pp. 40–42, 2016.

[33] C. Hou, *Ground Control of Roadways*, China University of Science and Technology Press, Xuzhou, China, 2013.